

POROSITY CALIBRATION OF MODERN POROSITY LOGS AND OLD NEUTRON LOGS,
MABEE FIELD, ANDREWS AND MARTIN COUNTIES, TEXAS

DENNIS W. DULL
TEXACO EXPLORATION AND PRODUCTION INC.

ABSTRACT

As a part of the reservoir characterization and for calculation of original oil in place, it is necessary to correct the porosity logs to the core data. The Mabee field has 800+ logs with a majority of them consisting of old gamma ray neutron logs.

The modern porosity logs were calibrated to core porosity by crossplotting log porosity against core porosity. Linear regressions were constructed which are defined by the slope and the y-intercept. The linear regressions demonstrated excellent linear correlation. It was observed that location of the well or geology appears to be more important in the relationship between core porosity and log porosity than the logging company. A logging company utilizing the same tool and logging boreholes the same size across the field exhibited varying slopes and y-intercepts. Conversely, one well logged by two different companies obtained nearly identical linear regressions. Maps of slopes and y-intercepts were used to obtain the transforms for converting modern porosity logs to core porosity. The cased hole neutron porosity logs indicated that location was important, but that the logging company was equally as important. The slopes and y-intercepts were mapped by logging company.

The old neutron logs demonstrated a good inverse linear relationship between core porosity and the \log_{10} of the neutron deflection. Linear regressions were done for the \log_{10} neutron deflection vs. core porosity over the gross pay. Linear regressions of the mean and maximum \log_{10} neutron deflection vs. the mean and field minimum porosity generated nearly identical slope and y-intercept. Thus, any of the neutron deflection curves could be transformed to porosity if the mean porosity was known. Mean porosities were mapped using all core and transformed porosity logs over gross pay. These contoured values of mean porosity were used to generate a slope and y-intercept that would define the transform to convert \log_{10} neutron deflection to porosity.

INTRODUCTION

The Mabee field is one of three fields currently targeted for enhanced oil recovery utilizing CO_2 by Texaco in the Permian Basin (Figure 1). The purpose of the individual CO_2 groups was to provide an accurate reservoir description that would not only support the past history of the field, but would predict future reservoir performance and

recoveries along with providing for the monitoring of the CO₂ miscible flood after its initiation.

One of the major tasks in the reservoir description was to determine the original oil in place utilizing all available log and core data. The purpose of this paper is to describe the method which was used to calibrate modern porosity logs to core and to normalize old neutron logs in order to obtain reservoir height or PHI*H.

The Mabee field has 650+ old neutron logs of which about 75 cannot be used at all because they were stimulated with nitroglycerine. The Mabee field also has about 150 modern porosity logs. In addition, approximately 85 wells have been cored at the Mabee field, of which only 35 wells have the core report and no actual core for description. All of the logs and core data have been digitized. Before the logs were sent out for digitization, all pertinent information such as logging company, tool model no., hole size, casing point, casing size and weight, source to detector spacing, etc. were recorded and entered on to a spreadsheet to be used in calibrating the logs to core porosity.

The log analysis, mapping, and data base management necessary to obtain PHI*H were done on a personal computer. It could not have been accomplished within the incurred time constraints without it.

GEOLOGY

The Mabee field discovered in October, 1943 covers an area of 12,800 acres and is located east of the Central Basin platform in the central portion of the Midland basin. (Figure 1). The Mabee field produces from the San Andres Formation of Permian Guadalupian Age. Although isolated from similar San Andres production, the favorable reservoir facies was draped over paleostructure/topography of Early Pennsylvanian age.

The Mabee field has produced over 90 million barrels of oil and is currently producing about 8,000 BOPD. The San Andres production is from a dolomite reservoir, a time-transgressive sequence that prograded from southwest New Mexico southward across the Midland basin (Todd, 1976).

The San Andres of the Mabee field is composed of six distinct facies typical of a sabkha type environment such as found in the present day Persian Gulf.

The six facies are: Supratidal (anhydrite rich, permeability barrier responsible for trapping the oil), Oncolites/Pisolites Subtidal, Ooid, Sandstone, and Open Marine. The productive sequence is almost exclusively confined to the subtidal and ooid facies.

The reservoir at the Mabee field has been divided into three zones (Figure 2). Zone 1 is capped by a very thin clay-rich stratigraphic

marker known as the "B". It is easily identified on the logs by its characteristic high radioactive gamma ray response. Below the "B" marker is the supratidal facies, composed of dolomite, nodular anhydrite, and stromatolitic lamina. Below the supratidal facies is a mixture of subtidal mudstone to wackestone to peloid packstones and subtidal oolite packstone to grainstones. Zone 2 is composed of primarily a sandstone and ooid facies. The sandstone facies, except on rare occasions when porosities reach 15% is impermeable, non-reservoir rock. The sandstone facies can be generally identified on the logs by its associated high gamma ray response when compared to the clean, low gamma ray of the ooids. Zone 3 is dominated by the ooid facies, vuggy porosity, solutioning, fractures, and high porosities and permeabilities. Zone 3 typically produces high volumes of water with significant H₂S.

Zone 3 has produced considerable amounts of oil, but because of the high porosities and permeabilities will not be flooded because of the potential for thieving of the CO₂. The interval to be flooded, gross pay, as used in this paper averages 115' in thickness and consists of Zones 1 and 2 and excludes the sandstones. See Figure 2.

LOG ANALYSIS

The log analysis was completed in two steps utilizing those cores and logs over gross pay. The first step was the analysis of the modern porosity log versus core porosity. The second, was to establish a relationship between core porosity and old neutron log deflection.

NEUTRON-DENSITY LOGS

Log analysis software was used to crossplot core porosity (COREPOR) against neutron-density crossplot porosity (PND). See Figure 3. The regression work indicated that a first degree polynomial fit the data best (Figure 4). In other words, there was a linear relationship between neutron-density crossplot porosity and core porosity. Individual plots of COREPOR versus PND were made for 16 wells over gross pay. Equations of the line, slope and y-intercept, along with correlation coefficients were generated using the log analysis software (Figure 5). (NOTE: For statistical purposes, it is extremely important that the interval be large enough to be significant and correlative from well to well.)

The results of the linear regressions are shown in Table 1. All of the wells exhibit a high correlation coefficient (a correlation coefficient of 1.00 would indicate a perfect linear correlation). With the exception of A-1 #483, all wells were used in calibrating the PND curves to core. Well A-1 #483 has an anomalously low slope, but high correlation coefficient. This is believed to be the result of drilling with oil base mud, while all the other wells were drilled with brine.

Logging Company A used the same neutron and density tools, with the exception of A-1 #574 which had a slightly different neutron tool. The linear regression slopes varied from 0.708 to 0.996. The y-intercepts varied from 0.009 to 0.206. Company B also demonstrated similar variability even though using the same logging tools. Despite the variability in slope and y-intercept, the linear regressions had a high correlation coefficient.

This variability in slopes and y-intercepts is attributed to the changes in geology (lithology, porosity types and percentages) and changes in salinity due to waterflooding with fresh water. In other words, the slopes and y-intercepts are more of a function of where the wells are drilled than the logging company. An example of this is Well A-4 #69 logged by companies A and B. The linear regressions generated slopes and y-intercepts that are very close. See Table 1.

If geology or location is the controlling factor, then mapping of the slopes and y-intercepts should reflect a gradual change across the field when contoured. In addition, slopes and y-intercepts should be predictable. Figures 6 and 7 are the maps of the slopes and y-intercepts of the linear regression of core porosity versus neutron-density crossplot porosity. Well A-1 #648 was cored and logged after the map was constructed. The map predicted a slope of 0.86 and a y-intercept of 0.014. Table 1 shows the actual slope and y-intercept to be 0.88 and 0.018, respectively.

DENSITY POROSITY VERSUS CORE POROSITY

Linear regression analysis was accomplished using the log analysis software for density porosity on a dolomite matrix of 2.87 g/cm^3 versus the core porosity. This was done for two reasons. First, was to verify that the density porosity had a good correlation with core porosity since the San Andres at the Mabee field is a known dolomite reservoir. Second, the logging tools were stacked with the neutron tool on top leaving the bottom portion of the pay section with only the density porosity. See Figure 8. No rathole was obtained for logging because of the high water volumes encountered when drilling into Zone 3 and its high H_2S content.

Figures 9 and 10 show the crossplot of the density porosity (PDDOL) against core porosity (COREPOR) and the statistical output of the regression analysis. Table 2 shows the slopes and y-intercepts of the linear regressions and their associated correlation coefficients for density porosity versus core porosity for 16 wells. The linear regressions showed a good correlation of density porosity when crossplotted with core porosity. Figures 11 and 12 show the gradual change of slope and y-intercept of the linear regressions across the field. As was found with neutron-density crossplot porosity versus core porosity, the slopes and y-intercepts are controlled more by where the well was drilled or geology than logging company. Again, A-4 #69 had similar slopes and y-intercepts for both logging companies A and B. See Table 2. In addition, as with the slopes and y-

intercepts of the A-1 #648 of the neutron-density crossplot porosity versus core porosity, the linear regression of density porosity crossplotted against the core porosity had a slope and y-intercept very close to the predicted value from the maps. The predicted values of slope and y-intercept from the contoured values were 0.725 and 0.011 with the actual being 0.765 and 0.012.

CASED HOLE NEUTRON POROSITY VS. CORE POROSITY

The cased hole neutron porosity analysis did not exhibit the same relationship as the open hole porosity logs. Well A-4 #69 was logged by four different logging companies. Linear regressions of log porosity on a dolomite matrix (PNDOLCH) versus core porosity (COREPOR) were done. The slopes and y-intercepts show a significant difference. See Table 3. Notice that all companies have a high correlation coefficient indicating a good linear response for each company's calculation of porosity. See Figures 13-16. It appears from this that the logging company does make a significant difference in the relationship between core and cased hole neutron log porosity. Therefore, mapping of slopes and y-intercepts regardless of logging company to convert log porosity to core porosity would not be possible. However, mapping slopes and y-intercepts by logging company would be a solution providing there is enough core and wells logged by a specific company. Figures 17 and 18 are the maps of the slopes and y-intercepts of Logging Company D.

TRANSFORMING LOG POROSITY TO CORE POROSITY

The log porosities were transformed to core porosity by using the slope and y-intercept for the contoured values and applying that transform to that specific well. In other words, instead of one transform for all the wells logged by a specific logging company, there would be a different transform for every well. To verify the accuracy of the transform, the pseudocore porosity was compared to the actual core porosity for all wells used in the analysis. See Figure 19.

Once this relationship had been established, the transforms were obtained from the maps and used to convert the log porosity to pseudocore porosity of any well in the field.

In regards to the cased hole porosity logs, there was only one well, logged by Company D, that went through gross pay. The maps of y-intercept and slope of Company D were the only ones necessary to convert its log porosity to pseudocore porosity. Table 4 shows the PHI*H of the cored wells to their core transforms.

OLD NEUTRON LOGS

The converting of log porosity to pseudocore porosity was necessary if any attempt to accurately convert the old neutron logs to porosity. The more core data, the better the control of porosity that could be

applied to the old neutron logs. The ideal way to transform old neutron logs to core porosity is to have a core in every well, obviously that situation usually does not exist. However, there were 13 wells over gross pay with core and logged with old neutron logs.

The relationship between neutron log deflection and porosity was demonstrated by Brown and Bowers (1959). They discovered that there is an inverse linear relationship between porosity and the \log_{10} of the neutron deflection measured from neutron zero. In Figure 20 an example of this relationship is shown.

In calibrating their neutron logs at SACROC (Swulius, 1986) discovered that he could use statistical descriptors in place of the entire core to obtain the same transform. Those statistical descriptors were the maximum, minimum and mean of core porosities vs. \log_{10} deflections. The most unreliable descriptor was the relationship of the \log_{10} of the minimum neutron deflection to maximum porosity, probably in part due to the low count rates in the high porosities.

Figures 21 and 22 show the linear regressions of two wells: using (1) core porosity vs \log_{10} deflection, (2) maximum, minimum, and mean values of core vs \log_{10} deflection, (3) mean and minimum of the log porosity vs mean and maximum of \log_{10} deflection, (4) mean and 0.015 (field minimum) porosity vs. mean and maximum of \log_{10} deflection.

The two examples demonstrate that using field minimum porosity or minimum porosity and mean porosity vs. the mean and maximum of the \log_{10} neutron deflection nets nearly the same result as using all the core data vs. the log data. In other words, the statistical descriptors worked as well as if all the data had been used. The significance of this, providing there is ample core data, is that the mapping of the mean porosity across the field would allow the calibration of any old neutron log to core regardless of logging company, tool model no., hole size, cased or open hole, etc. providing the neutron log is over gross pay. Table 5 presents the results of the regression of the 13 wells of core porosity vs. \log_{10} deflection. Table 5 demonstrates as Figures 21 and 22 illustrate that using the statistical descriptors of core (mean and minimum) is sufficient for obtaining the slope of the line, therefore, the transform for converting \log_{10} deflection to porosity providing logs are over gross pay. Figure 23 is the map of mean porosity over gross pay (Zones 1 and 2) utilizing all core and pseudocore porosities.

There were 29 cores and 28 porosity logs employed in generating the mean porosity map. Of the 29 cores, 16 wells had both core and modern open hole porosity logs and 15 had cased hole neutron porosity logs. Thirteen wells had core porosity over gross pay with old neutron deflection curves.

All neutron logs over gross pay were transformed to porosity by crossplotting mean and maximum of \log_{10} neutron deflection against the mean (obtained from contoured value on the map Figure 23) and field

minimum porosity (0.015). This generated a regression equation which then was applied to the \log_{10} of the neutron deflection curve to transform it to porosity. Figure 24 shows well #105 which compares core porosity, core transform porosity, and pseudocore transform porosity (using maximum and mean \log_{10} neutron deflection vs 0.015 and mean porosity of the core data to generate an algorithm for neutron log transformation to porosity). Well #105 shows excellent agreement between the core transform porosity (TPNEU1) and transform porosity (TPNEU2).

SUMMARY AND CONCLUSIONS

- (1) The neutron-density and density porosity demonstrated an excellent linear correlation to core porosity that depended more on where the well was drilled than the logging company.
- (2) The relationship of neutron-density and density porosity to core porosity for any one logging company varies in the Mabee field reflecting changes in geology.
- (3) The cased hole neutron porosity log response displayed a good linear response to core porosity, but indicated a dependence on logging company.
- (4) The linear correlation of the cased hole neutron porosity log to core porosity for any one logging company varied across the field as did the neutron-density logs mirroring changes in lithology.
- (5) The neutron-density, density, and cased hole neutron porosity logs were transformed to pseudocore porosity utilizing the maps of the slopes and y-intercepts of the linear regressions of log porosity crossplotted against core porosity.
- (6) The old neutron logs exhibited an inverse linear response of the \log_{10} neutron deflection when crossplotted against core porosity.
- (7) The statistical descriptions of mean and field minimum porosity (0.015) crossplotted versus the mean and maximum \log_{10} neutron deflection generated nearly the same slope and y-intercept of the linear regression as applying all the core and log data.
- (8) The mapping of the mean porosity from the cores and the transformed porosity logs would enable the generation of a transform to convert \log_{10} neutron deflection over gross pay to porosity.

ACKNOWLEDGMENTS

The author thanks Texaco for permission to publish this paper. He is grateful to the CO₂ Department, Midland Producing Division for the encouragement and support in assembling this paper. The author also wishes to acknowledge Lois Folger for her assistance in the analysis of the old neutron logs and to Tekla Dupuis for her help in producing the maps and log data base.

BIBLIOGRAPHY

- Bebout, D. G. and P. M. Harris, Eds., 1990, Geologic and Engineering Approaches in Evaluation of San Andres/Grayburg Hydrocarbon Reservoirs - Permian Basin, Bureau of Economic Geology.
- Brown, A. A. and B. Bowers, 1957, The Relationship Between Neutron Log Deflection and Porosity, CWLS, Canadian Symposium Papers 1, No. 39, p. 39-43.
- Ghosh, S. K. and G. M. Friedman, 1989, Petrophysics of a Dolostone Reservoir: San Andres Formation (Permian), West Texas, Carbonates, and Evaporites, V. 4, p. 45-119.
- Swulius, T. M., 1986, Porosity Calibration of Neutron Logs, SACROC Unit, Journal of Petroleum Technology, April, p. 468-476.
- Todd, R. G, 1976, Oolite-bar Progradation, San Andres Formation, Midland Basin, Texas: AAPG Bulletin, V. 60, p. 907-925.

Table 1
Neutron Density Crossplot Porosity (PND)
vs.
Core Porosity

Well No.	Y-Intercept	Slope	Correlation Coefficient	No. Samples	Logging Company
A-1 483	.020	.615	.94	170	C
" 538	.025	.915	.90	129	B
" 539	.017	.838	.73	131	B
" 574	.002	.820	.94	170	A
" 597	.033	.803	.84	172	A
" 599	.023	.931	.93	183	A
" 601	.009	.943	.96	154	A
" 603	.021	.996	.95	186	A
" 604	.013	.836	.94	163	A
" 610	.026	.825	.90	69	A
" 616	.014	.848	.94	175	A
" 624	.009	1.007	.97	153	B
" 643	.012	.881	.95	115	A
" 648	.018	.880	.95	158	A
A-4 69	.020	.708	.95	74	A
" 69	.027	.715	.96	68	B
" 71	.006	.909	.93	154	B

Table 2
Density Porosity - Dolomite Matrix (PDDOL)
vs.
Core Porosity

Well No.	Y-Intercept	Slope	Correlation Coefficient	No. Samples	Logging Company
A-1 483	.026	.489	.88	141	C
" 538	.015	.679	.92	123	B
" 539	.017	.788	.72	165	B
" 574	.009	.763	.88	155	A
" 597	.026	.710	.80	145	A
" 599	.016	.888	.93	182	A
" 601	.009	.806	.93	151	A
" 603	.010	.760	.92	169	A
" 604	.013	.752	.86	208	A
" 610	.013	.718	.80	145	A
" 616	.004	.781	.92	200	B
" 624	-.010	.932	.96	154	B
" 643	.006	.720	.83	87	A
" 648	.012	.765	.94	152	A
A-4 69	.015	.725	.898	148	A
" 69	.017	.715	.93	130	B
" 71	.011	.808	.89	148	B

Table 3
Cased Hole Compensated Neutron Porosity -
Dolomite Matrix (PNDOLCH)
vs.
Core Porosity

Well No.	Y-Intercept	Slope	Correlation Coefficient	No. Samples	Logging Company
A-1 538	.041	.922	.80	121	C
" 539	.058	.600	.69	159	E
" 574	.039	.682	.91	152	D
" 594	-.013	.711	.85	192	B
" 599	.025	.642	.91	182	D
" 601	.028	.775	.91	125	D
" 603	.025	.890	.92	212	A
" 604	.032	.772	.91	205	D
" 610	.036	.819	.91	101	D
" 616	.027	.813	.92	207	D
" 624	.017	.924	.94	158	D
" 643	.028	.706	.92	150	D
" 648	.027	.723	.91	162	D
A-4 69	.035	.924	.94	184	A
" 69	.044	.730	.91	182	B
" 69	.047	.955	.92	170	C
" 69	.031	.517	.94	158	D
" 71	.032	.510	.88	153	D

Table 4
Comparison of PHI*H from Core and Transformed Logs

Well No.	LOG	CORE	LOGGING COMPANY
A-1 483	7.407	7.465	C
538	6.660	6.553	B
539	9.248	9.118	B
574	6.242	6.221	A
597	8.229	8.216	A
599	10.403	10.004	A
601	6.184	6.138	A
603	8.071	8.345	A
604	11.142	10.613	A
610	9.061	9.217	A
616	9.002	8.929	B
624	7.283	7.225	B
643	3.716	3.697	A
648	6.740	6.629	A
A-4 69	10.003	9.478	A
69	9.897	9.478	B
71	4.900	5.125	B

Table 5
Linear Regression Core Porosity vs. Log₁₀
Neutron Deflection

Well No.	All Core and Log Data				Logging Company	Number Samples	Mean and Field Minimum of Porosity		Mean and Minimum Core Porosity	
	Y-Intercept	Slope	Correlation Coefficient				Y-Intercept	Slope	Y-Intercept	Slope
A-1 105	1.947	-.595	.90		G	194	1.786	-.545	1.809	-.552
305	1.792	-.530	.86		F	180	1.707	-.504	1.707	-.504
356	1.245	-.354	.75		F	226	1.375	-.396	1.375	-.396
361	1.570	-.464	.88		F	221	1.419	-.419	1.419	-.416
380	1.726	-.507	.75		G	249	1.945	-.574	1.739	-.511
481	1.528	-.449	.89		F	229	1.629	-.480	1.455	-.426
488	0.747	-.243	.71		F	222	0.574	-.183	0.590	-.189
494	1.143	-.347	.89		F	220	1.206	-.368	1.206	-.368
495	1.185	-.368	.90		F	226	1.114	-.344	1.114	-.344
503	0.911	-.298	.87		F	253	0.745	-.240	0.745	-.240
A-3 18	1.136	-.328	.93		F	229	0.899	-.257	1.017	-.292
B-1 26	1.127	-.365	.73		F	249	1.180	-.383	1.167	-.379
MFC 12	1.047	-.277	.84		F	181	0.869	-.228	0.869	-.228

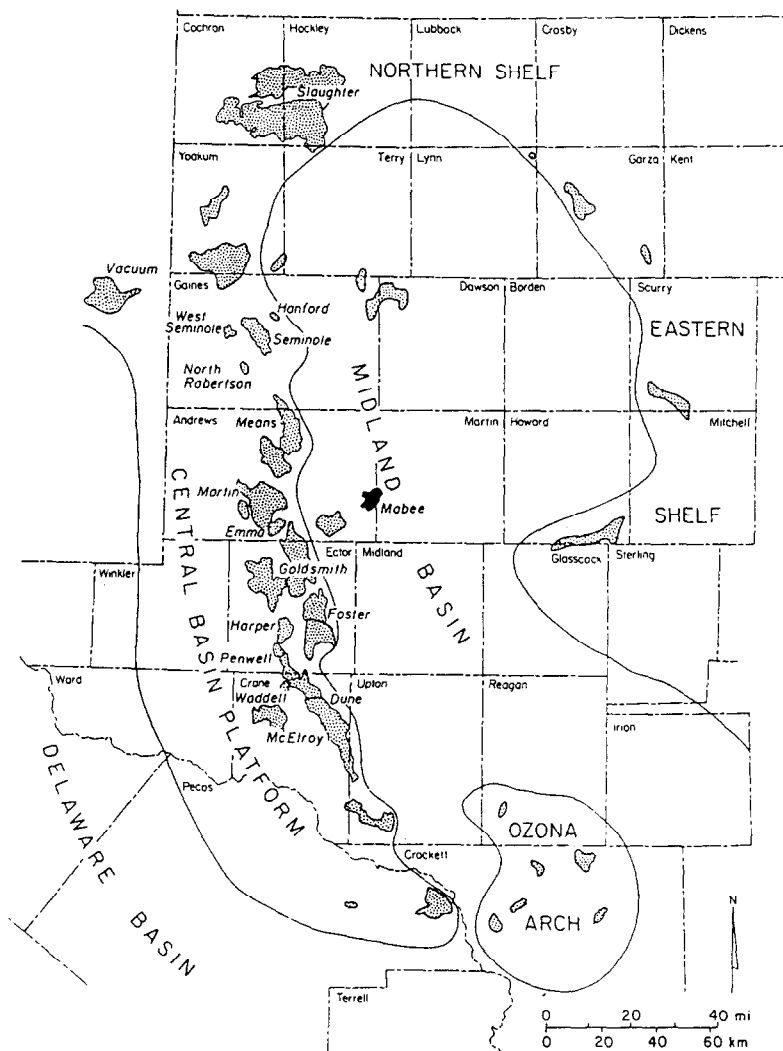


Figure 1 - Map of a portion of the Permian Basin showing the location of the Mabee Field in the western-central part of the Midland Basin (from Bebout and Harris, 1990)

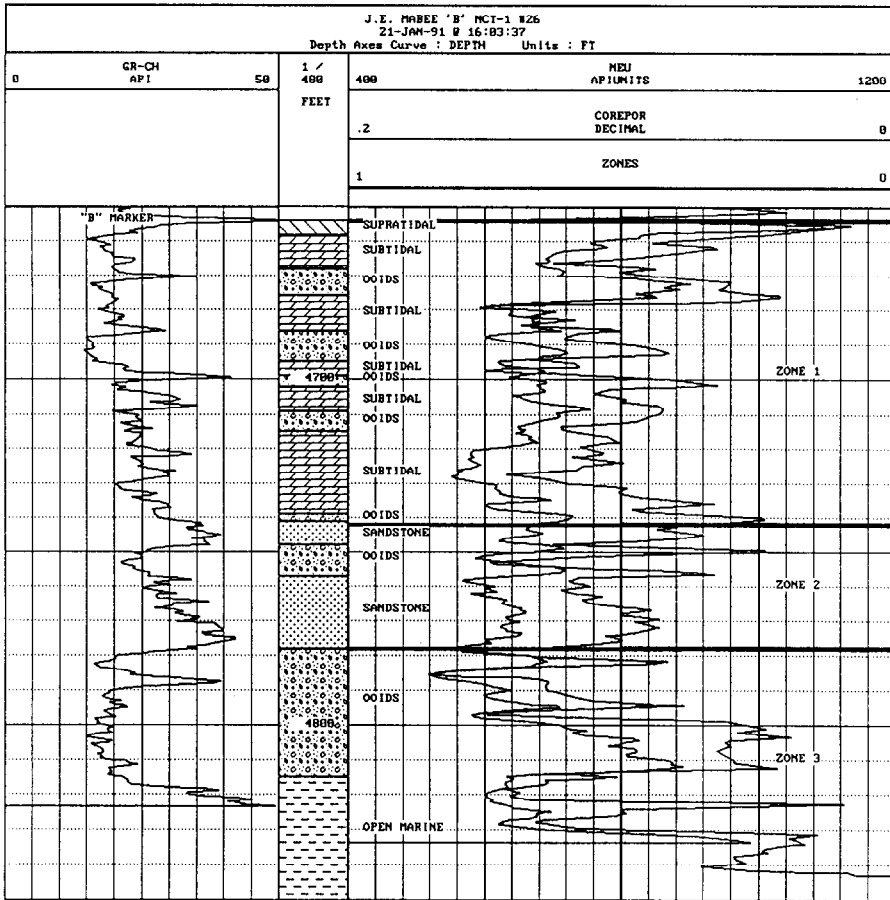


Figure 2 - Type log for the San Andres showing the diversity of the facies and Zones 1, 2 and 3

WELL : (3) J.E. MABEE "A" NCT-1 #604 AW,WDC
DATE : 25-JAN-91 @ 07:04:04
ZONE : 4687.00 - 4778.00 FT

X: PND DECIMAL Y: COREPOR DECIMAL

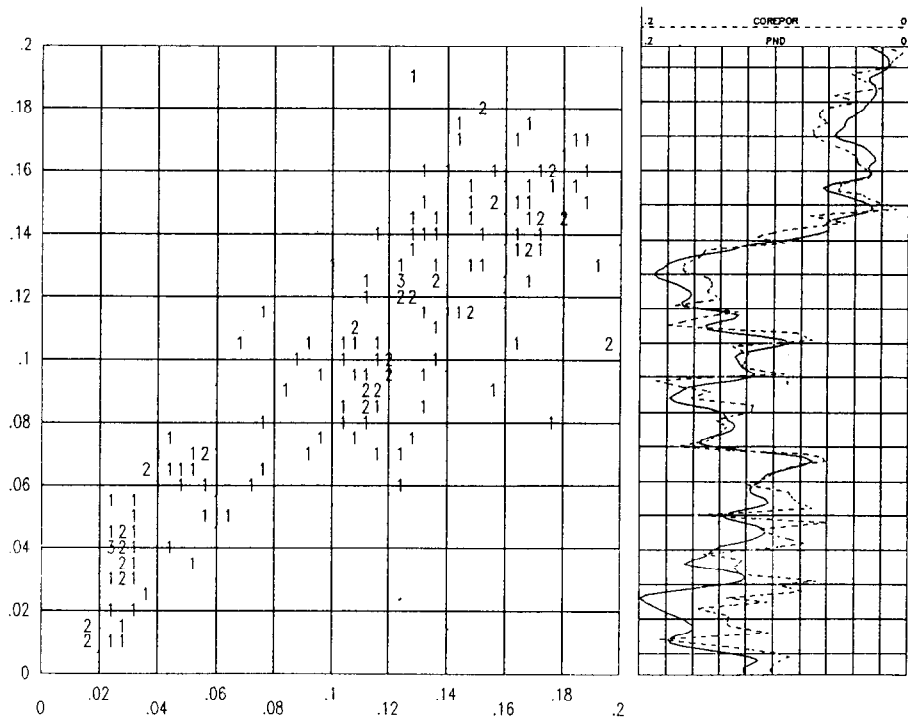


Figure 3 - Crossplot of the neutron-density crossplot porosity (PND) vs. the core porosity (COREPOR). Note: The numbers on the crossplots indicate the number of values in a particular cell on the graph.

WELL : (3) J.E. MABEE "A" NCT-1 #604 AW,WDC
 DATE : 25-JAN-91 @ 07:04:04
 ZONE : 4687.00 - 4778.00 FT

X: PND DECIMAL Y: COREPOR DECIMAL

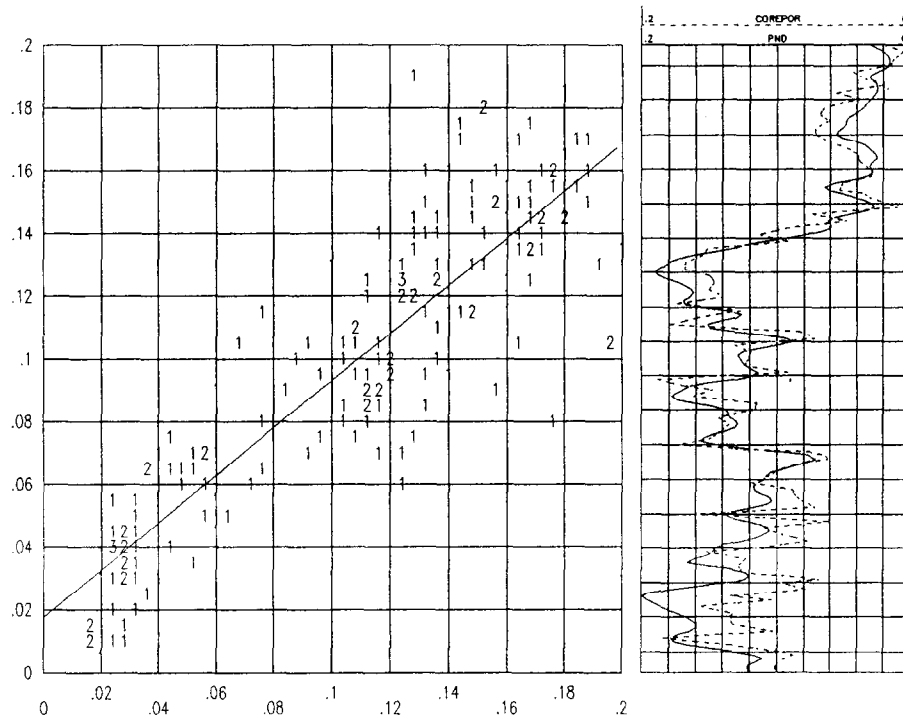


Figure 4 - Crossplot, log and linear regression of the neutron-density crossplot porosity (PND) vs. core porosity (COREPOR) for the J. E. Mabee 'A' NCT-1 #604

WELL : (3) J.E. MABEE "A" NCT-1 #604 AW,WDC
 ZONE : 4687.00 - 4778.00 FT
 DATE : 18-JAN-91 @ 09:25:36

Color Crossplot Regression Analysis

Crossplot Parameters: (183 points plotted)

curve name	axis scale values	no. null values	no. exceeded scales
X-AXIS = PND	.000 to .200	0	0
Y-AXIS = COREPOR	.000 to .200	0	0

Discriminators: (.0 points failed discriminator test)

none
 Drop value = none

Degree = 1
 Correlation Coefficient = .93936
 $Y = .12519021E-01 * X^{**0} + .82686811 * X^{**1}$

Regression Results: (165 samples) X on Y

Figure 5 - Statistical output of the linear regression analysis of the neutron-density crossplot porosity (PND) vs. core porosity (COREPOR) from the log analysis software for the J. E. Mabee 'A' NCT-1 #604

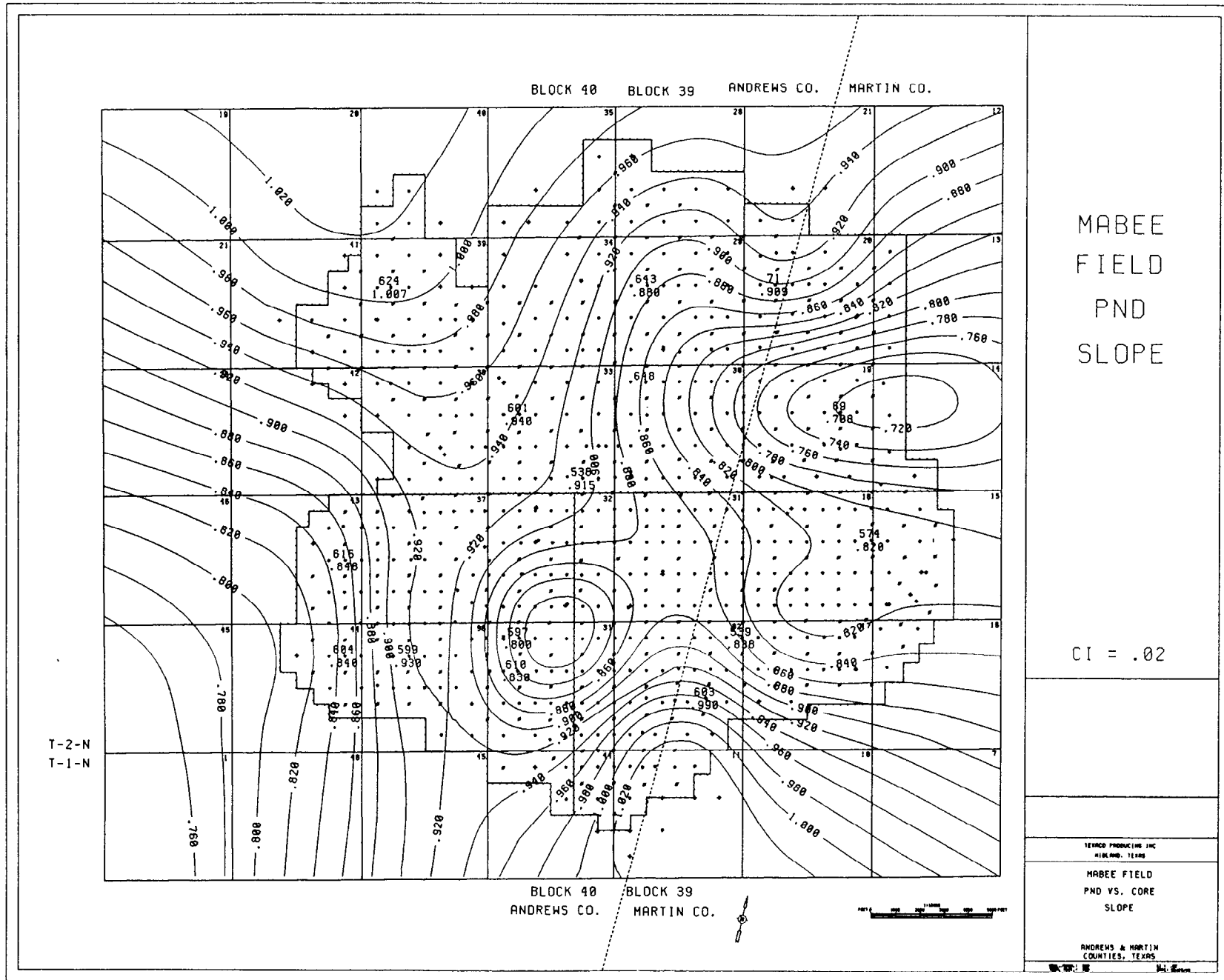


Figure 6 - Map of the slope of the linear regression of neutron-density crossplot porosity (PND) vs. core porosity over gross pay

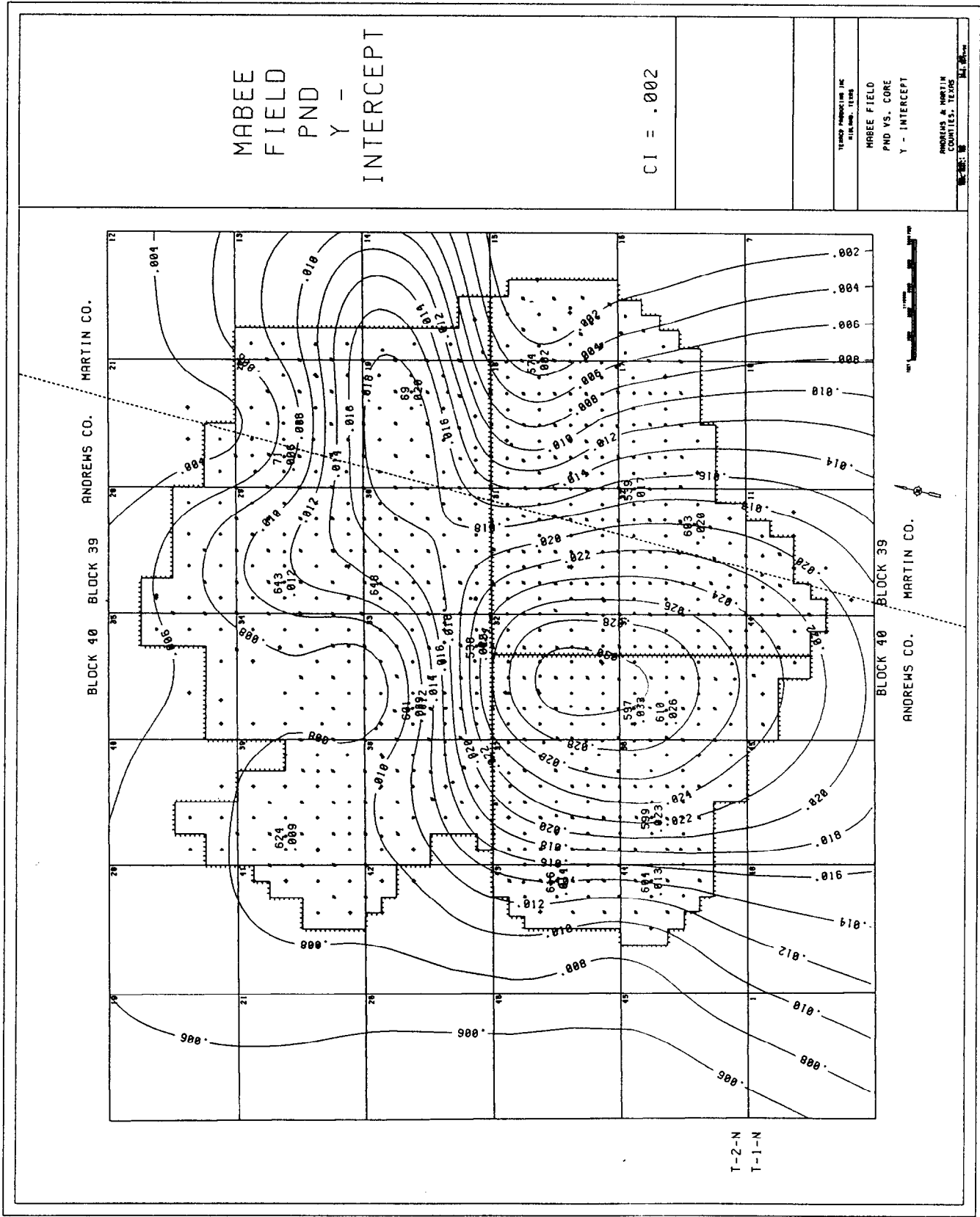


Figure 7 - Map of the y-intercept of the linear regression of the neutron-density crossplot porosity (PND) vs. core porosity over gross pay

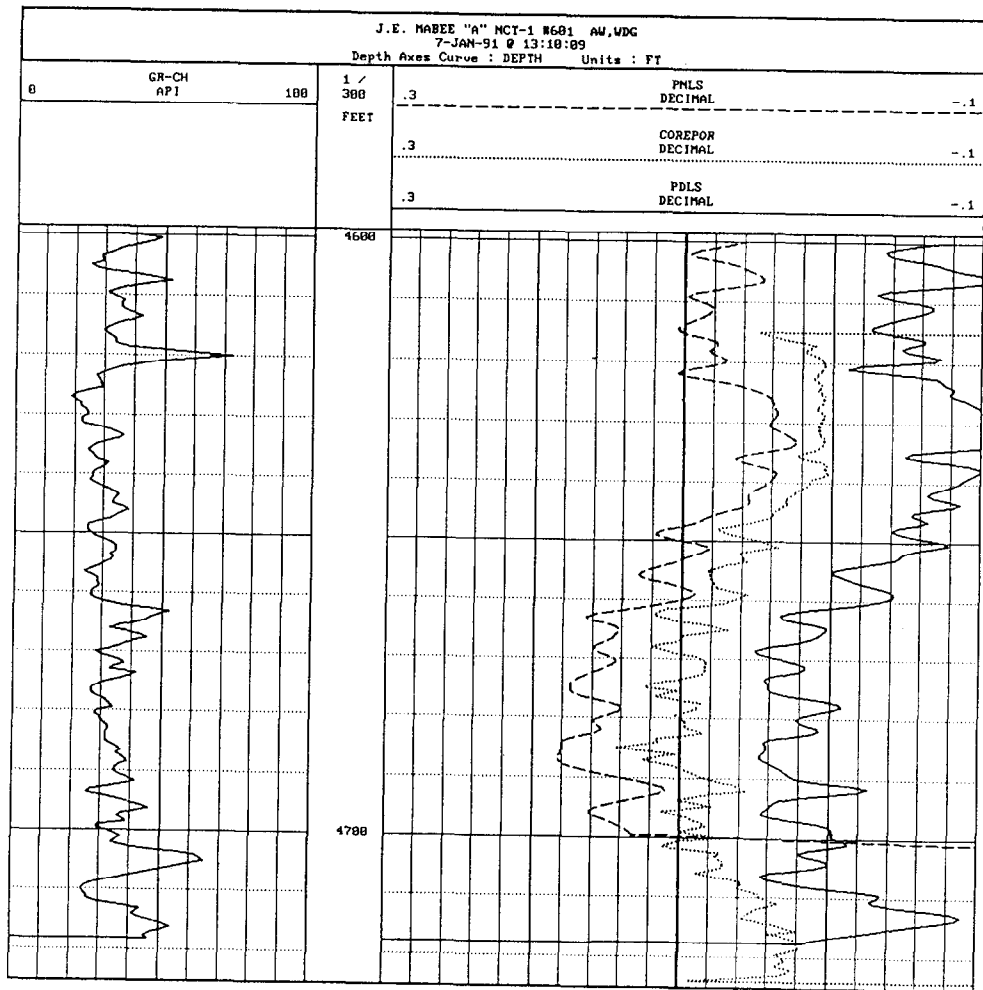


Figure 8 - Log showing the neutron porosity not going to TD. (PNLS-
neutron porosity limestone matrix, PDLS-density porosity
limestone matrix, COREPOR-core porosity)

WELL : (103) J.E. MABEE 'A' NCT-1 #616 HLS,WDG
 DATE : 9-JAN-91 @ 15:07:55
 ZONE : 4662.00 - 4767.00 FT

X: PDDOL DECIMAL Y: COREPOR DECIMAL

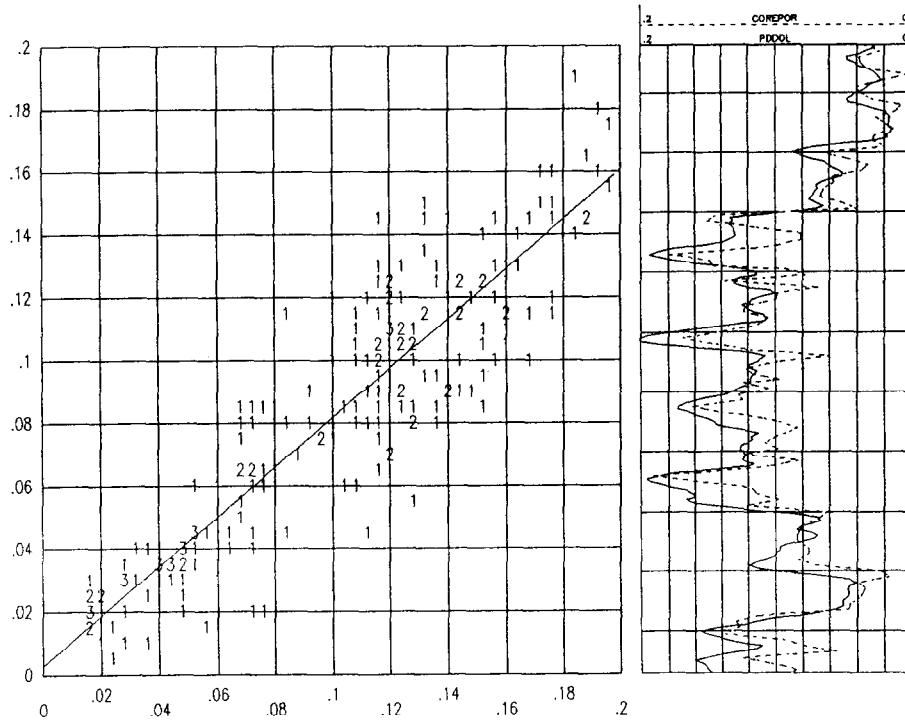


Figure 9 - Crossplot, log, and linear regression of the density porosity-dolomite matrix (PDDOL) vs. core porosity (COREPOR) for the J. E. Mabee 'A' NCT-1 #616

WELL : (103) J.E. MABEE 'A' NCT-1 #616 HLS,WDG
 ZONE : 4662.00 - 4767.00 FT
 DATE : 18-JAN-91 @ 09:11:13

Color Crossplot Regression Analysis

Crossplot Parameters: (209 points plotted)

curve name	axis scale values	no. null values	no. exceeded scales
X-AXIS = PDDOL	.000 to .200	0	2
Y-AXIS = COREPOR	.000 to .200	0	0

Discriminators: (0 points failed discriminator test)

none
 Drop value = none

Degree = 1
 Correlation Coefficient = .91998
 $Y = .35503441E-02 * X^{*0} + .78830624 * X^{*1}$

Regression Results: (202 samples) X on Y

Figure 10 - Statistical output of the regression analysis of the density porosity-dolomite matrix (PDDOL) vs. core porosity (COREPOR) from the log analysis software for the J. E. Mabee 'A' NCT-1 #616

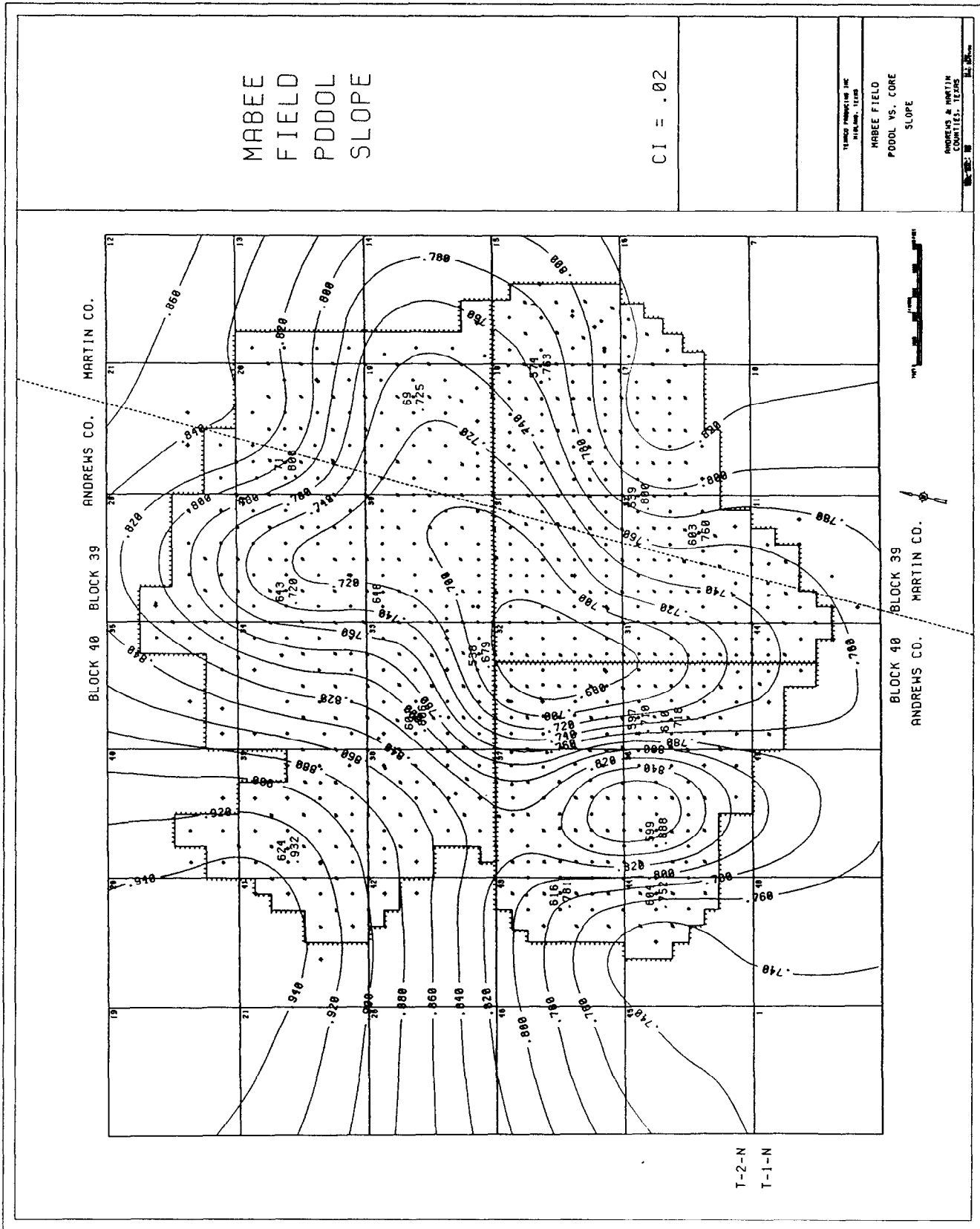


Figure 11 - Map of the slope of the linear regression of the density porosity on a dolomite matrix (PDDOL) vs. core porosity over gross pay

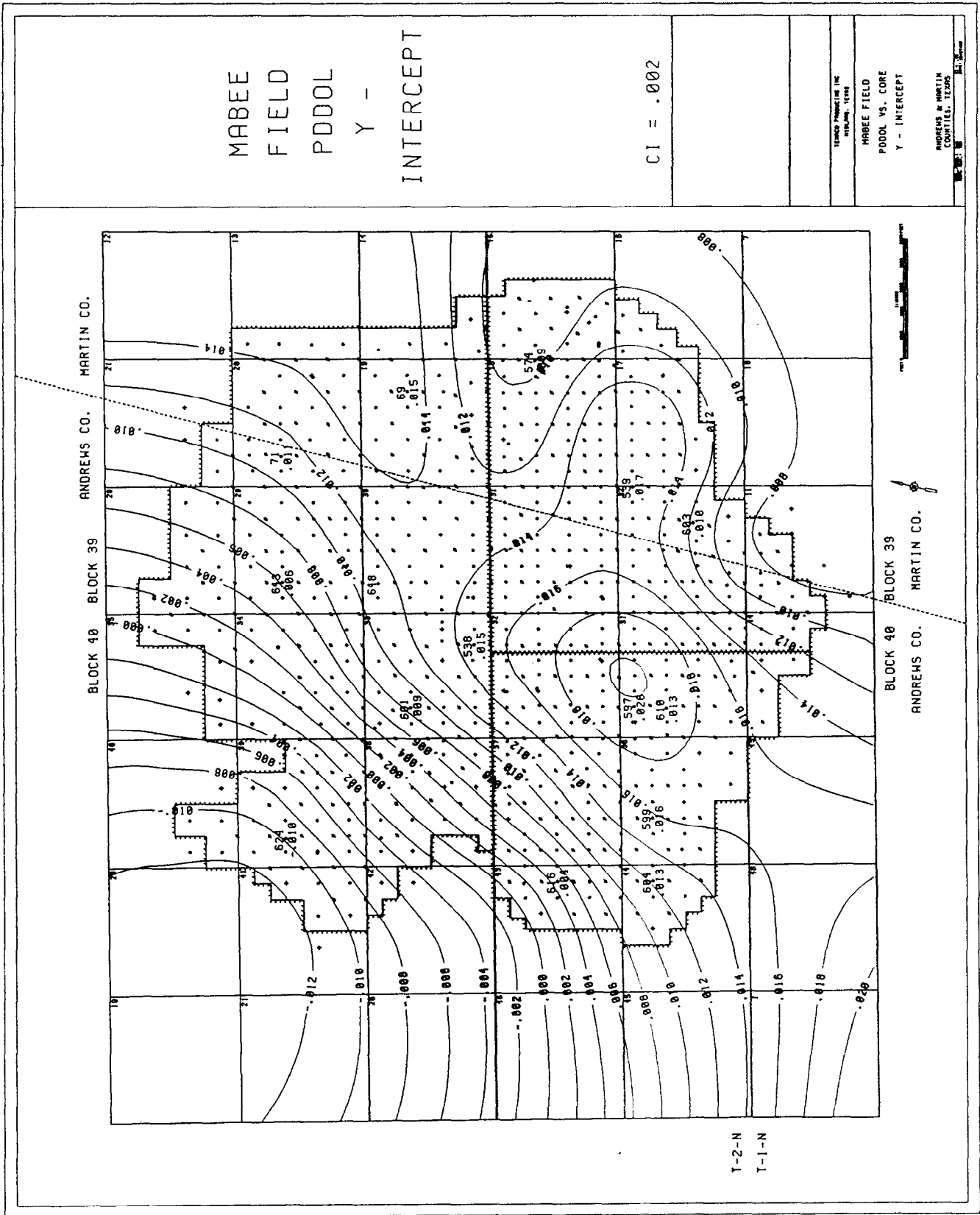


Figure 12 - Map of the y-intercept of the linear regression of the density porosity on a dolomite matrix (PDDOL) vs. core over gross pay

WELL : (134) J.E. MABEE 'A' NCT-4 #69 AW,AW
 DATE : 28-DEC-90 @ 11:24:15
 ZONE : 4675.00 - 4772.00 FT

X: DSPNDOLC DEC Y: COREPOR DECIMAL

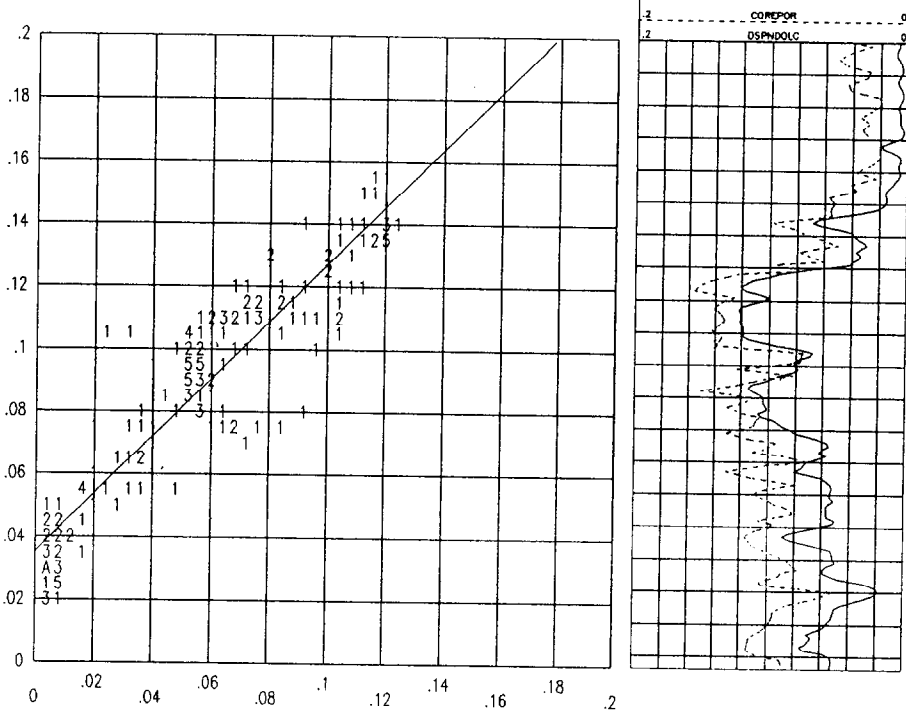


Figure 13 - Crossplot, log, and linear regression of the cased hole neutron porosity-dolomite matrix (PNDOLCH) vs. core porosity (COREPOR) for Company A of the J. E. Mabee 'A' NCT-4 #69

WELL : (128) J.E. MABEE 'A' NCT-4 #69 HLS,HLS
 DATE : 28-DEC-90 @ 11:15:07
 ZONE : 4672.00 - 4772.00 FT
 DISCRIMINATORS: <= CPFLAG <= 1
 X: PNDOLCH DEC Y: COREPOR DEC

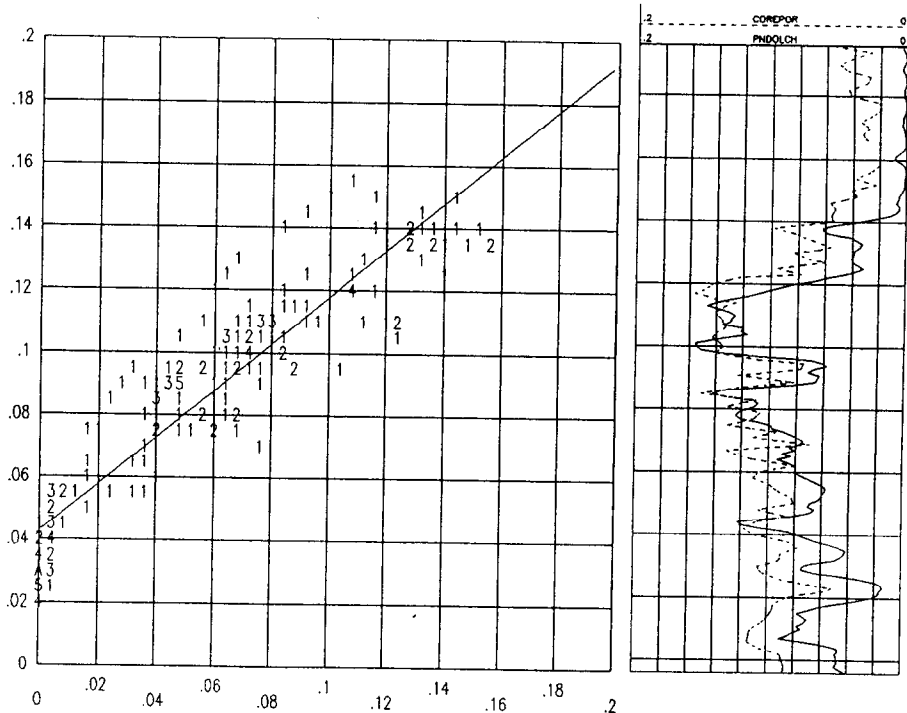


Figure 14 - Crossplot, log, and linear regression of the cased hole neutron porosity-dolomite matrix (PNDOLCH) vs. core porosity (COREPOR) for Company B of the J. E. Mabee 'A' NCT-4 #69

WELL : (129) J.E. MABEE 'A' NCT-4 #69 SWS,SWS
 DATE : 28-DEC-90 @ 10:53:21
 ZONE : 4678.00 - 4772.00 FT
 DISCRIMINATORS: <= CPFLAG <= 1
 X: PNDOLCH DEC Y: COREPOR DEC

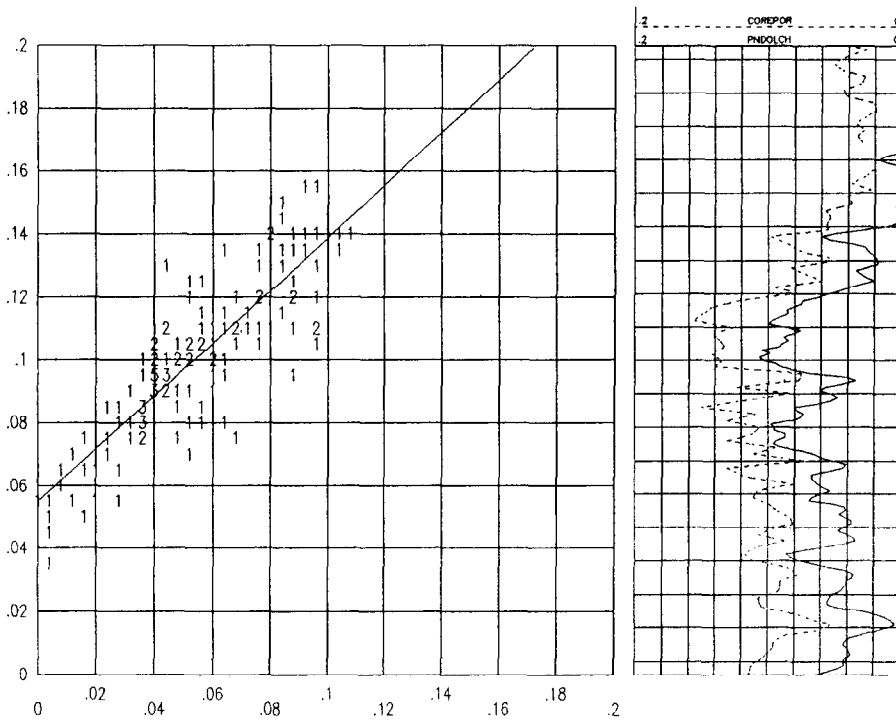


Figure 15 - Crossplot, log, and linear regression of the cased hole neutron porosity-dolomite matrix (PNDOLCH) vs. core porosity (COREPOR) for Company C of the J. E. Mabee 'A' NCT-4 #69

WELL : (139) J.E. MABEE 'A' NCT-4 #69 WDG
 DATE : 28-DEC-90 @ 11:04:16
 ZONE : 4675.00 - 4772.00 FT
 DISCRIMINATORS: <= CPFLAG <= 1
 X: PNDOLCH DEC Y: COREPOR DEC

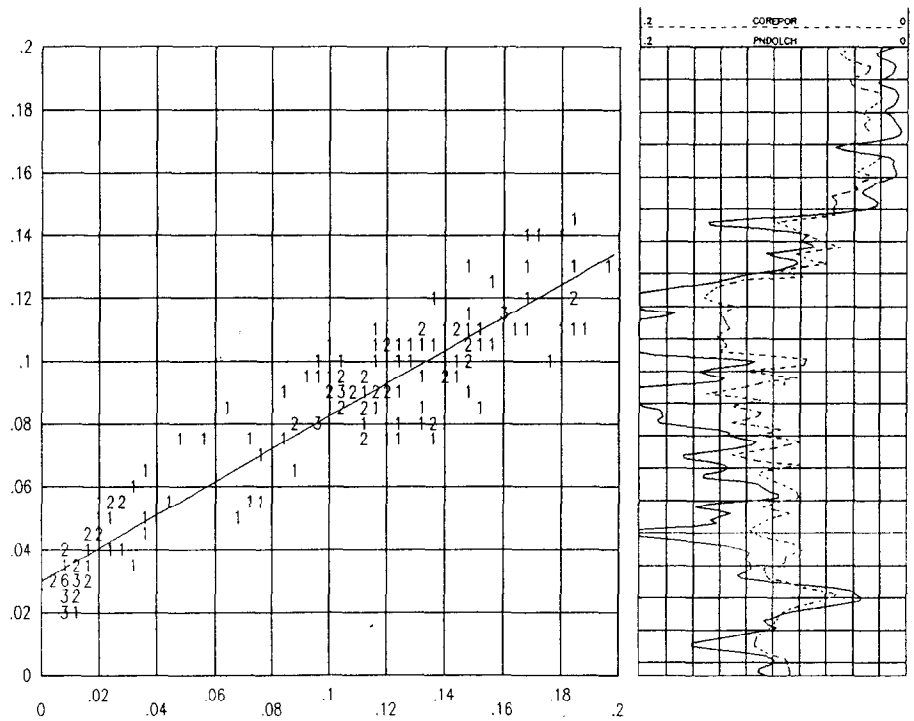


Figure 16 - Crossplot, log, and linear regression of the cased hole neutron porosity-dolomite matrix (PNDOLCH) vs. core porosity (COREPOR) for Company D of the J. E. Mabee 'A' NCT-4 #69

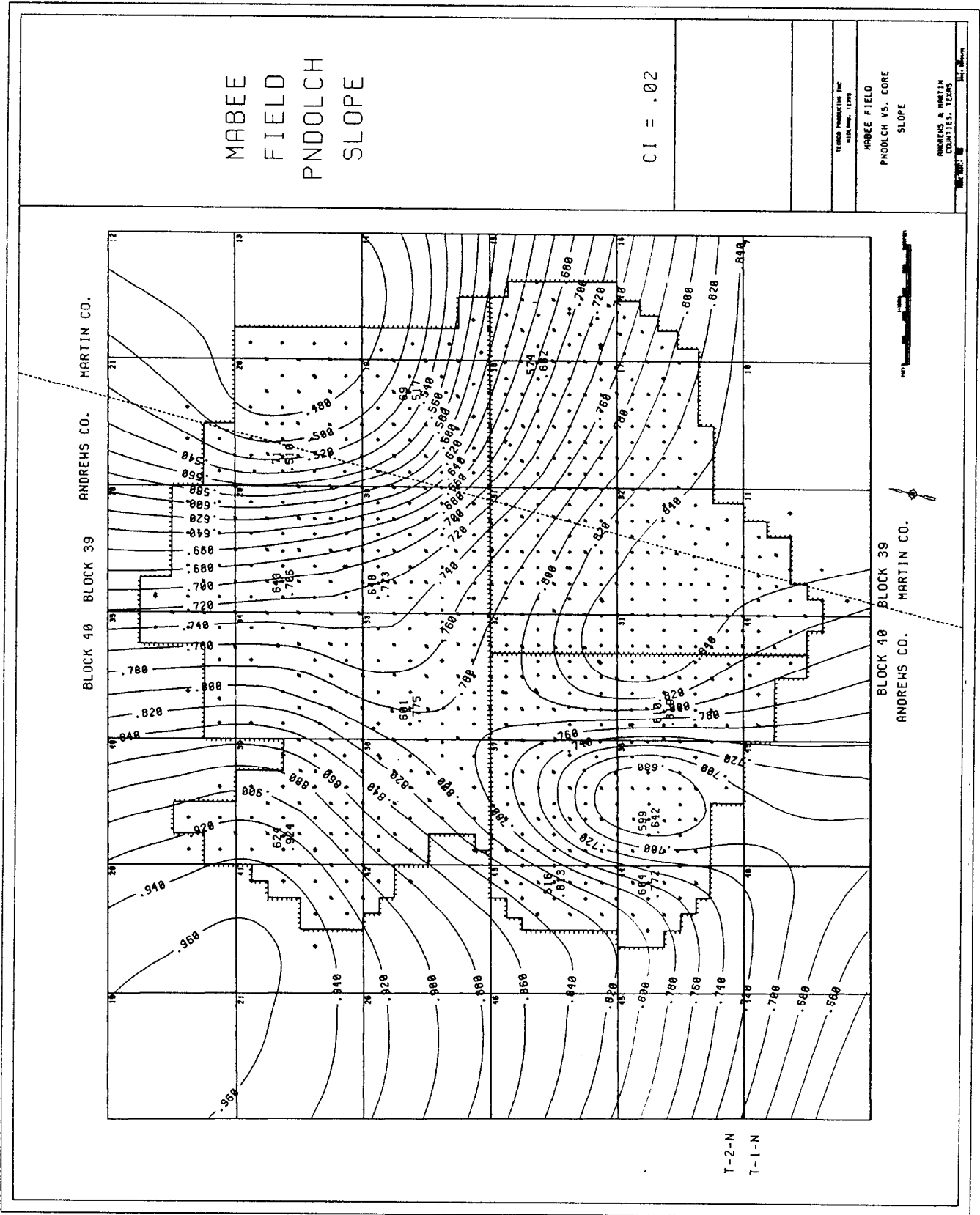


Figure 17 - Map of the slope of the linear regression of the cased hole neutron porosity-dolomite matrix (PNDOLCH) vs. core porosity over gross pay (Company "D" only)

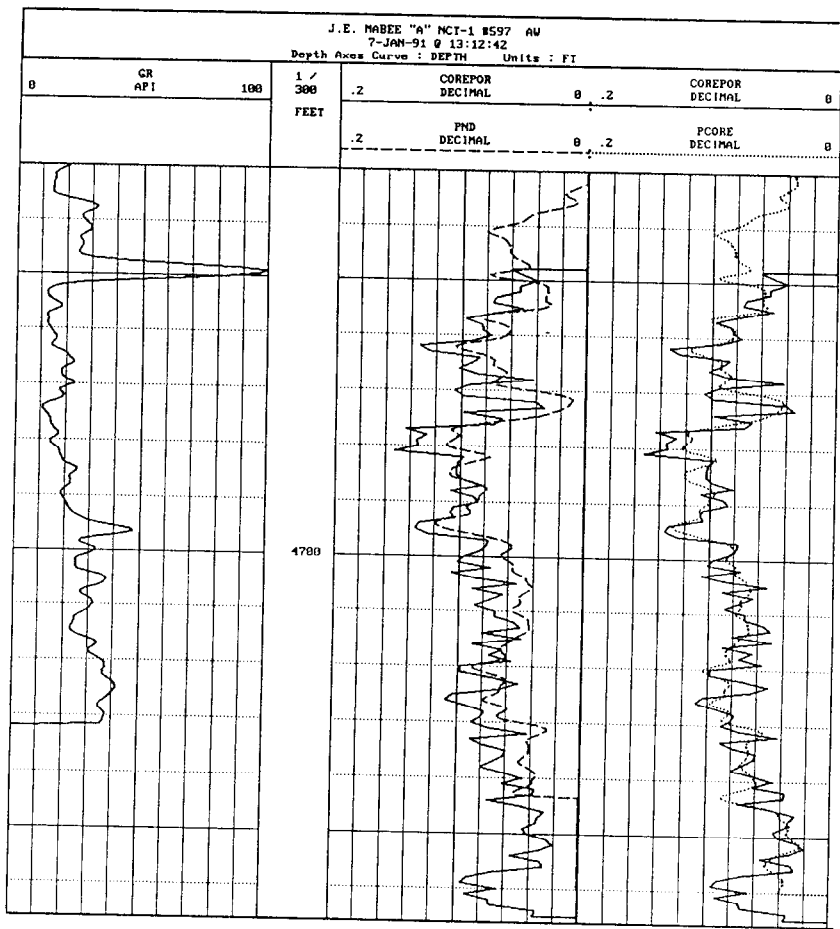


Figure 19 - Log illustrating the improvement of the transformed neutron-density cross-plot porosity (PCORE, pseudocore porosity) vs. core porosity (COREPOR) over the neutron-density cross-plot porosity (PND) for the J. E. Mabee 'A' NCT-1 #597

WELL : (7) J.E. MABEE 'A' NCT-1 #105
DATE : 24-JAN-91 @ 11:56:22
ZONE : 4623.00 - 4720.00 FT

X: LOGNEU DECIMAL Y: COREPOR DECIMAL

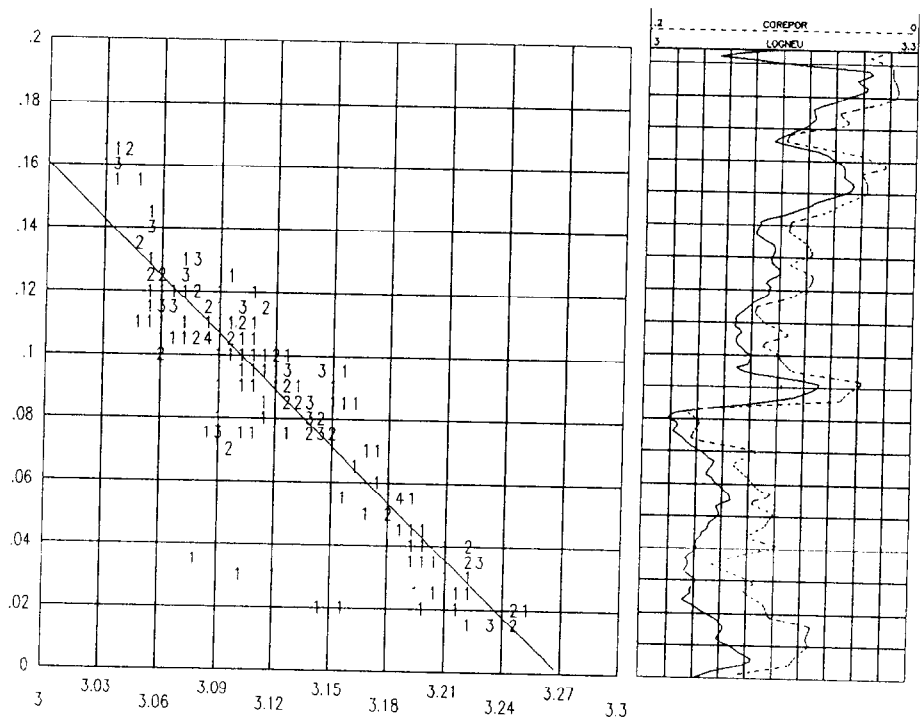


Figure 20 - Crossplot, log, and linear regression of the \log_{10} of the neutron deflection (LOGNEU) vs. the core porosity (COREPOR) of the J. E. Mabee 'A' NCT-1 #105 illustrating the inverse linear relationship

LOG(NEUTRON) VS. CORE POROSITY J.E. MABEE 'A' NCT-1 NO. 105

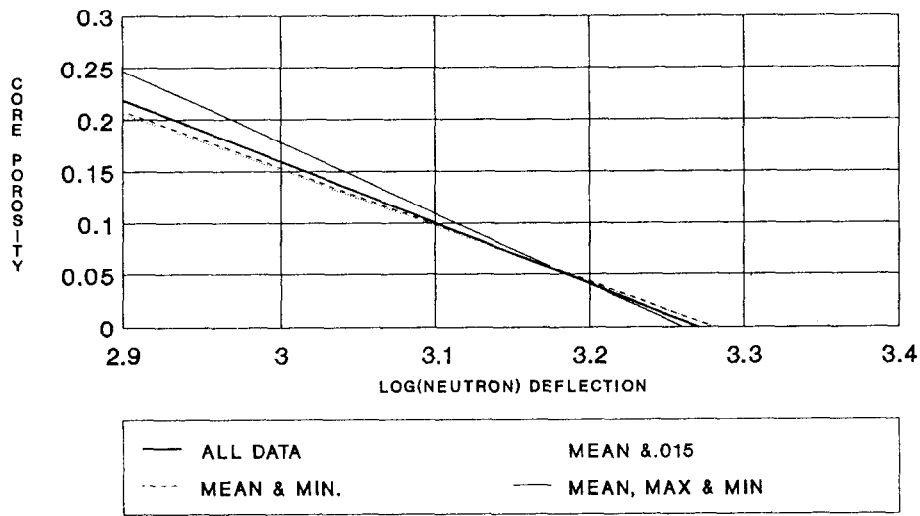


Figure 21 - A comparison of the linear regressions of the statistical descriptors with all the core and log data

LOG(NEUTRON) VS. CORE POROSITY J.E. MABEE 'A' NCT-1 NO. 494

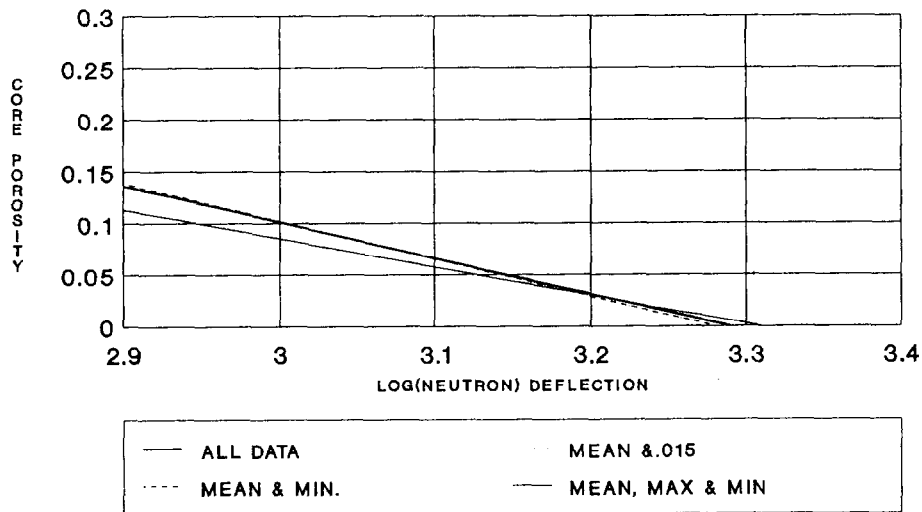


Figure 22 - A comparison of the linear regressions of the statistical descriptors with all the core and log data

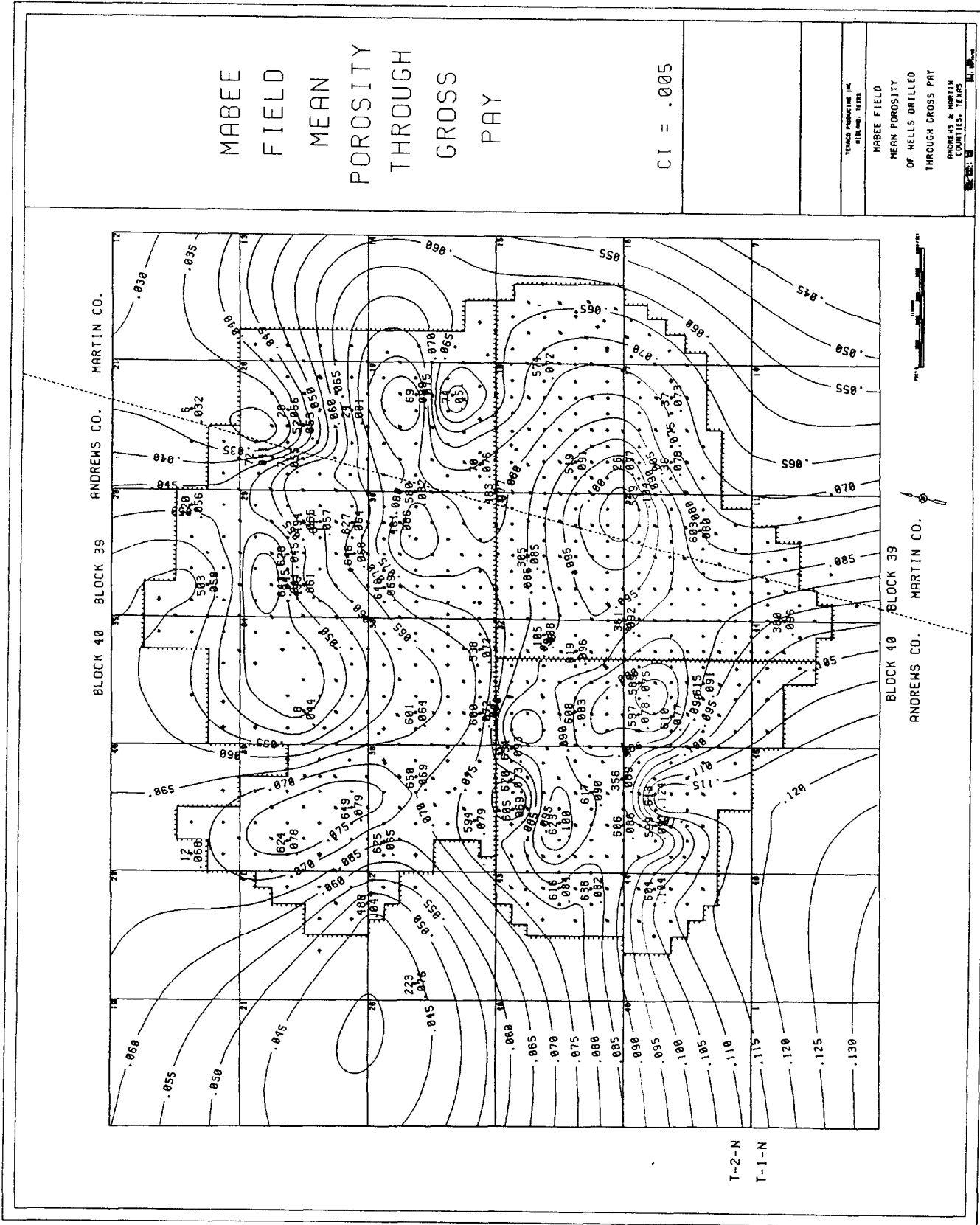


Figure 23 - Map of the mean porosity of the wells drilled through gross pay (cores and porosity logs)

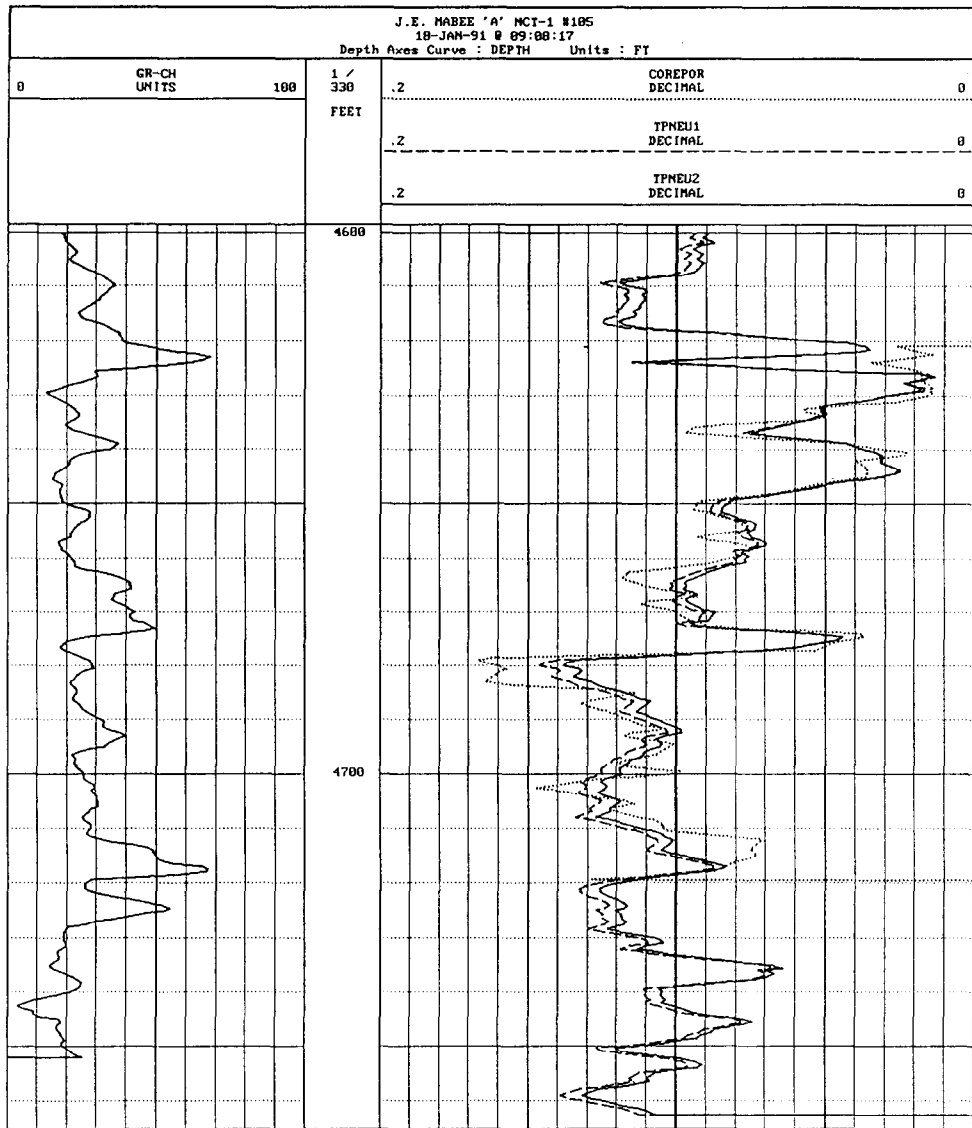


Figure 24 - Log illustrating the difference between the two log transforms using all the core and log data (TPNEU1) and the mean and field minimum porosity of 0.015 (TPNEU2). Note: Both transforms closely follow the core porosity (COREPOR)